

INCREASE IN GRAIN BOUNDARY CONDUCTIVITY OF $\text{Li}_{1+x}\text{Al}_x\text{Sn}_{2-x}(\text{PO}_4)_3$ BY MIXING POWDERS PRETREATED AT DIFFERENT TEMPERATURES

#XIAOJUAN LU, HUINING XIAO

*School of Environmental Science and Engineering, North China Electric Power University,
Mailbox 253, No.689 Huadian Road, Baoding, Hebei, P. R. China*

#E-mail: xiaojuanlv@hotmail.com

Submitted June 1, 2016; accepted September 7, 2016

Keywords: Ionic conductors, NASICON, Grain boundaries, Mixture

The overall conductivity of crystalline lithium ion conductors is generally low due to the large grain boundary resistance. In order to improve the grain boundary conductivity, NASICON structured $\text{Li}_{1+x}\text{Al}_x\text{Sn}_{2-x}(\text{PO}_4)_3$ has been studied in this paper. Samples $\text{Li}_{1.2}\text{Al}_{0.2}\text{Sn}_{1.8}(\text{PO}_4)_3$ with the desirable amount of Al, made of a mixture of not-treated powders and treated powders in various ratios, are prepared to investigate the mixing effect on the grain boundary conductivity. The grains morphology of samples has changed from spherical shapes to rectangular shapes upon mixing, which indicates a liquid (or glass) phase formation during sintering. The overall conductivity peaks at 20 % of not-treated powders. The increase in the overall conductivity is attributed to the increase of grain boundary conductivity, not the grain conductivity. The reason accounting for the enhancement of the grain boundary conductivity is attributed to a less-resistive grain boundary as indicated by the grains morphology changes observed.

INTRODUCTION

The standard lithium-ion battery has been the leading energy storage device since the mid 1990s due to its high power densities and long cycle life. A source of the high power density of the Li ion battery is its high operation voltage (~ 3.8 V), under which, water used as an electrolyte in most batteries, is decomposed into hydrogen and oxygen. Thus, flammable liquid organic electrolytes with a greater toleration to such high voltages must be used instead to avoid inherent safety issues, such as explosion. But organic liquid electrolytes still suffer from the disadvantages of flammability, safety concerns, leakage, corrosion and miniaturization difficulty.

To solve this safety problem, solid state lithium ion conductors have been extensively studied in the last decades for their application in lithium batteries [1-9]. Current researches show that crystalline materials with a NASICON (Na SuperIonic CONductor) structure, are promising candidates to replace organic liquid electrolytes. System $\text{Li}_{1+x}\text{Al}_x\text{Ge}_{2-x}(\text{PO}_4)_3$ (LAGP) [10-11], $\text{Li}_{1+x}\text{Al}_x\text{Ti}_{2-x}(\text{PO}_4)_3$ [3,4,6,11,12] and $\text{Li}_{1+x}\text{Al}_x\text{Zr}_{2-x}(\text{PO}_4)_3$ [13-14] were investigated by various research groups, among which LAGP exhibits conductivities in the range of 10^{-3} - 10^{-4} S \cdot cm $^{-1}$ and appears to be the most stable. Polycrystalline materials, however, generally have low overall conductivity due to the large grain boundary resistance, which is normally one order of magnitude higher than that of the grains. Intensive investigations

have been carried out to reduce the grain boundary resistance of crystalline materials, thus to improve the overall conductivity of lithium ion conductors. Methods to accomplish this improvement include the development of a glass-ceramic process and use of sintering to increase the density. Methods, including adding Si [12], excessive lithium [15], and etc, have also been tried by various groups since these second phases were believed to introduce some space charge layer, adjust compositions and modify the grain boundary, thus affect the ionic conductivity. These methods have been successful in some extent. But these dopants, in essence, are not ionic conductors, which could limit their effect to improve the ionic conductivity further.

Since polycrystalline lithium ion conductors are limited by the high grain boundary resistance, doping of some less crystallized counterpart into the system could help to introduce some intermediate phases into the grain boundary region, thus to reduce the grain boundary resistance. Apart from large grain boundary resistance, the use of expensive raw material of germanium in LAGP has prevented them from being of a real practical interest. Relatively cheap Sn, having the same valence as Ge $^{4+}$ and even bigger ionic radius which can increase the space for lithium ions to migrate, makes a possibly suitable candidate to replace Ge $^{4+}$. Thus, a series of $\text{Li}_{1+x}\text{Al}_x\text{Sn}_{2-x}(\text{PO}_4)_3$ materials with varied x has been prepared and efforts have been attempted to improve the grain boundary conductivity by mixing powders thermally treated at different temperatures in this study.

EXPERIMENTAL

A series of $\text{Li}_{1-x}\text{Al}_x\text{Sn}_{2-x}(\text{PO}_4)_3$ ($x = 0, 0.2, 0.4, 0.6$ and 0.8) materials has been prepared by solid state reaction method in this study. Li_2CO_3 ($\geq 99\%$), $\text{Al}(\text{OH})_3$ ($\geq 99\%$), SnO_2 ($\geq 99\%$) and $\text{NH}_4\text{H}_2\text{PO}_4$ ($\geq 99\%$) are starting materials and purchased from Sigma-Aldrich. Firstly, starting materials in stoichiometric ratio were weighed and mixed thoroughly in a pestle mortar for each composition. Secondly, all the mixtures were calcined at 700°C for 2 hrs to remove any volatile components and the resulting mixtures were assigned as not-treated powders (i.e. less crystallized powders). Thirdly, these not-treated powders were reground and pressed into pellets of 15 mm diameter using a press (769YP-24B, Tianjin Keqi Co. Ltd.) at a pressure of 10MPa, and then the pellets were sintered in a box furnace (Nanjing Kejing Co. Ltd.) at 900°C for 2 hrs (The heating/cooling rate was $3^\circ\text{C}\cdot\text{min}^{-1}$) to study the effect of the aluminum doping.

Once the optimal doping amount of Al has been acquired, above-mentioned not-treated powders of the optimal composition were thermally treated at 900°C for 2 hrs at a rate of $3^\circ\text{C}\cdot\text{min}^{-1}$ and the resulting powders were then reground to achieve treated powders of better sinterability. Then the not-treated powders, in different weight percentages of 10 %, 20 %, 30 %, 40 % and 50 %, were mixed with treated powders in a pestle mortar thoroughly. The mixture of not-treated and treated powders was pressed into pellets of 15 mm diameter using the press at a pressure of 10MPa and subsequently sintered at 800°C for 2 hrs at a heating/cooling rate of $3^\circ\text{C}\cdot\text{min}^{-1}$ to study the mixing effect.

All the sintered pellets were polished, painted with silver paste on both top/bottom sides and heated at 150°C for 1 h for electrochemical impedance spectra (EIS) analysis. The EIS measurements were carried out using a PARSTAT2273 station (Princeton Applied Research) by applying a stimulus amplitude of 10 mV over the frequency range of 0.1 Hz – 2×10^6 Hz at room temperature.

The microstructures were examined by using a field emission scanning electron microscope (JSM-7800F). Crystallographic phases analysis was carried out by X-ray diffraction with a D/max-2500J/pc diffractometer using a Cu K-radiation source ($\lambda = 0.15418$ nm). The density of the samples was determined by the Archimedes method using water as the immersion fluid.

RESULTS AND DISCUSSION

The effect of trivalent Al^{3+} doping

Trivalent Al^{3+} is widely doped to replace tetravalent ions in NASICON structured lithium ion conductors like $\text{LiGe}_2(\text{PO}_4)_3$ and $\text{LiTi}_2(\text{PO}_4)_3$ to improve the overall conductivity for several factors. The crystal structure

of NASICON materials consists of a three-dimensional rigid framework with MO_6 octahedra and PO_4 tetrahedra sharing common corners. Li^+ ions may occupy two interstitial positions: M1 sites of six fold coordination with oxygen atoms and M2 sites of eight fold coordination with oxygen atoms. Both sites alternate along the channels forming a three-dimensional conduction network. The different connectivity makes the relative occupancy of M1 and M2 sites a key factor to determine the ionic transport of the NASICON materials. When all the M1 sites are occupied by lithium, all the pathways for long-range ion motion are blocked by the own ionic carriers. The appropriate substitution of M^{4+} with trivalent ions like Al^{3+} , Fe^{3+} or Cr^{3+} promotes the occupancy of M2 sites, liberating part of the formerly blocked M1 sites and expanding the ionic conduction pathways, which improves the ionic conduction eventually. Additionally, it produces an increase in the carrier (Li^+) content in order to compensate the charge difference caused by the doping of trivalent ions. The enhancement on ionic conductivity is also attributed to the increase of density after incorporating of trivalent ions. For the same reason, aluminum amounts were varied in samples $\text{Li}_{1-x}\text{Al}_x\text{Sn}_{2-x}(\text{PO}_4)_3$ ($0 \leq x \leq 0.8$) to study the effect of Al doping in this paper. The relationship between total conductivity and Al doping amounts is shown in Figure 1. It can be seen that the total conductivity achieved as high as $2.46 \times 10^{-6} \text{ S cm}^{-1}$ which peaked at $x = 0.2$. This conductivity is higher than the value of Cr or Cr and V substituted $\text{LiSn}_2(\text{PO}_4)_3$ [16-17]. The total conductivities of $\text{Li}_{1-x}\text{Al}_x\text{Sn}_{2-x}(\text{PO}_4)_3$ ($0 \leq x \leq 0.8$) decreased with the Al doping amounts once x exceeded 0.2 and were all lower than the un-doped sample. Therefore, the optimal doping amount of Al is determined as 0.2 here for further investigations.

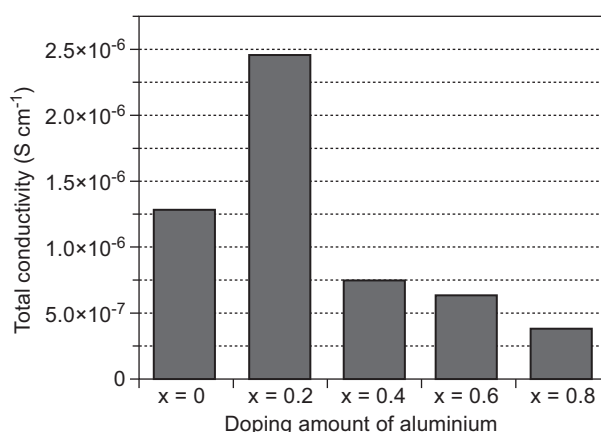
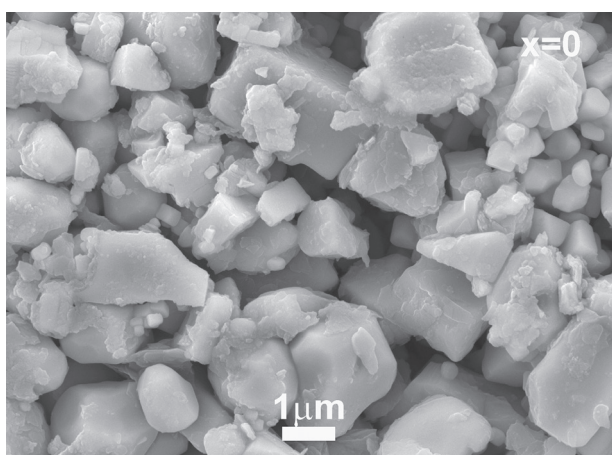


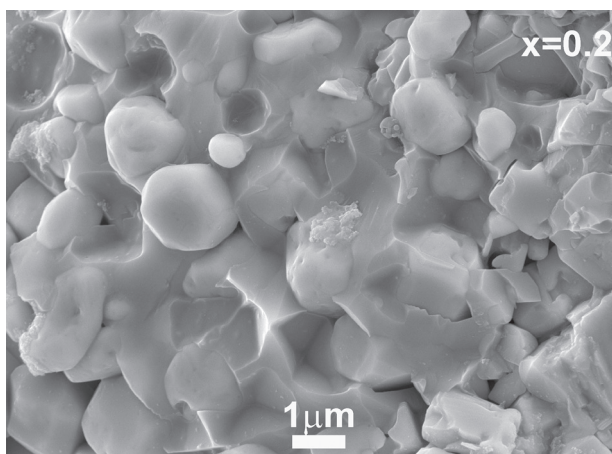
Figure 1. Total conductivities of samples $\text{Li}_{1-x}\text{Al}_x\text{Sn}_{2-x}(\text{PO}_4)_3$.

Figure 2 illustrates the SEM micrographs for the fractured cross-sections of $\text{LiSn}_2(\text{PO}_4)_3$ and $\text{Li}_{1.2}\text{Al}_{0.2}\text{Sn}_{1.8}(\text{PO}_4)_3$. It is evident that there was a change in morphology for un-doped $\text{LiSn}_2(\text{PO}_4)_3$ and doped $\text{Li}_{1.2}\text{Al}_{0.2}\text{Sn}_{1.8}(\text{PO}_4)_3$.

For un-doped $\text{LiSn}_2(\text{PO}_4)_3$, the particles were loosely gathered, while doped $\text{Li}_{1.2}\text{Al}_{0.2}\text{Sn}_{1.8}(\text{PO}_4)_3$ exhibited a very dense and well-packed structure with fewer pores. The relative density of sample $\text{LiSn}_2(\text{PO}_4)_3$ was measured as 75 % while the relative density of sample $\text{Li}_{1.2}\text{Al}_{0.2}\text{Sn}_{1.8}(\text{PO}_4)_3$ was measured as 80 %. It seems that the doping of Al helped to increase the density of the sample, which partially explains the increase of the conductivity observed as described previously. Another possible explanation for the enhanced conductivity could be attributed to an increase in the mobile Li^+ ion concentration as a result of charge compensation.



a)



b)

Figure 2. SEM micrographs of the fractured cross-sections of $\text{Li}_{1+x}\text{Al}_x\text{Sn}_{2-x}(\text{PO}_4)_3$.

As shown in Figure 3, X-ray diffraction examinations show that sample $\text{Li}_{1+x}\text{Al}_x\text{Sn}_{2-x}(\text{PO}_4)_3$ without Al doping has mixed phases of $\text{LiSn}_2(\text{PO}_4)_3$ (49-1175), SnP_2O_7 (29-1352) and SnO_2 (41-1445), among which phase SnP_2O_7 is the main phase instead of $\text{LiSn}_2(\text{PO}_4)_3$. While phase $\text{LiSn}_2(\text{PO}_4)_3$ started to dominate in the sample $\text{Li}_{1.2}\text{Al}_{0.2}\text{Sn}_{1.8}(\text{PO}_4)_3$, with minor traces of SnO_2 and SnP_2O_7 impurity. Beyond $x = 0.2$, some as-yet-unidentified phases appeared. The conductivity of

$\text{Li}_{1+x}\text{Al}_x\text{Sn}_{2-x}(\text{PO}_4)_3$ peaked at $x = 0.2$ as observed in Figure 1, which can be partially attributed to the phases transformation from impurity phases of SnP_2O_7 and SnO_2 to a desirable phase $\text{LiSn}_2(\text{PO}_4)_3$. The decreased conductivity is possibly attributed to the as-yet-unidentified phases formation as the doping of Al increased further.

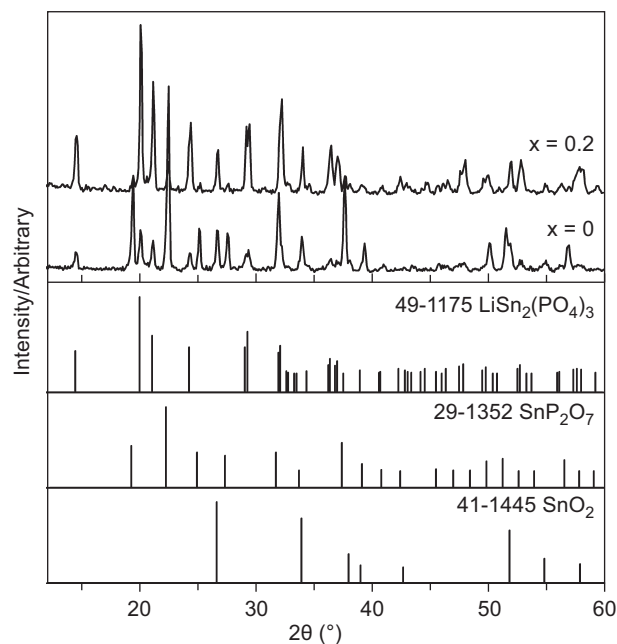


Figure 3. XRD patterns of $\text{Li}_{1+x}\text{Al}_x\text{Sn}_{2-x}(\text{PO}_4)_3$ ($x = 0, x = 0.2$).

The mixing effect of not-treated powders and treated powders

The main drawback of polycrystalline lithium ion conductors is the low grain-boundary conductivity. Heterogeneous dopants like Si could be detrimental to the properties of ionic conductors. Therefore homogenous dopants are introduced in this study as attempting to improve the ionic conductivity.

As the total conductivity of $\text{Li}_{1+x}\text{Al}_x\text{Sn}_{2-x}(\text{PO}_4)_3$ maximized at $x = 0.2$, composition $\text{Li}_{1.2}\text{Al}_{0.2}\text{Sn}_{1.8}(\text{PO}_4)_3$ is the study object in this section for determining the optimal mixing ratio of not-treated powders and treated powders. The mixing ratios of not-treated and treated powders were varied as 10 %, 20 %, 30 %, 40 % and 50 %. The total conductivity was plotted versus the mixing ratio of not-treated powders, shown in Figure 4. It was found that the plot of the total conductivity versus mixing ratio of not-treated powders exhibits as a parabolic curve. As seen in Figure 4, the total conductivity of samples increased as the mixing ratio of not-treated powders up to 20 %, and then it dropped when the mixing ratio exceeded 20 %. It maximized at 20 %, which shows that the total conductivity of $\text{Li}_{1.2}\text{Al}_{0.2}\text{Sn}_{1.8}(\text{PO}_4)_3$ can be enhanced by mixing a certain amount of less crystallized powders.

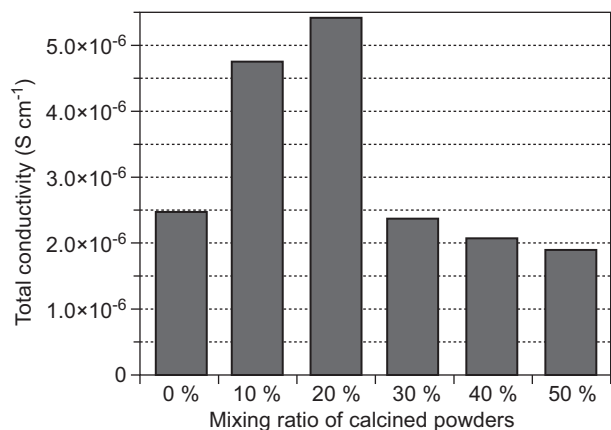
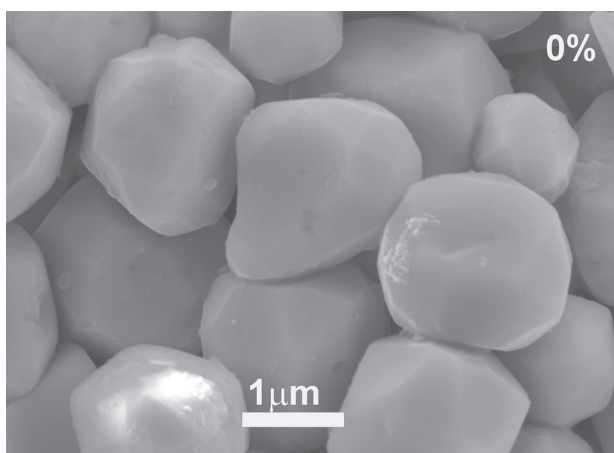
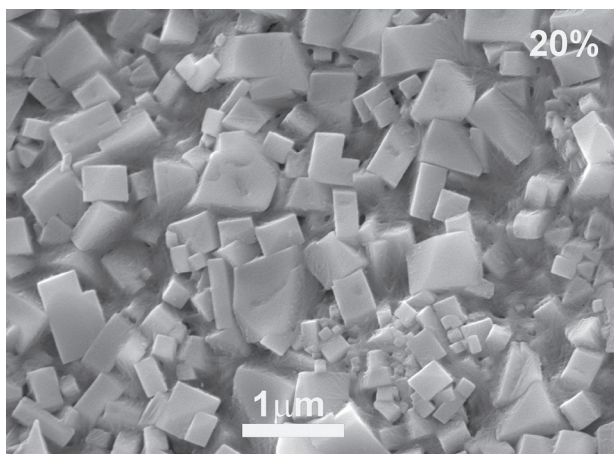


Figure 4. The total conductivity versus the mixing ratio of not-treated powders.

SEM photographs of $\text{Li}_{1.2}\text{Al}_{0.2}\text{Sn}_{1.8}(\text{PO}_4)_3$ made of 0 %, 20 % and 40 % of not-treated powders are shown in Figure 5. It is noticeable that the addition of not-treated powders made a very big difference on the morphology of samples $\text{Li}_{1.2}\text{Al}_{0.2}\text{Sn}_{1.8}(\text{PO}_4)_3$. The sample made of 0 % not-treated powders presented a relatively dense structure with well-defined grains in spherical



a)



b)

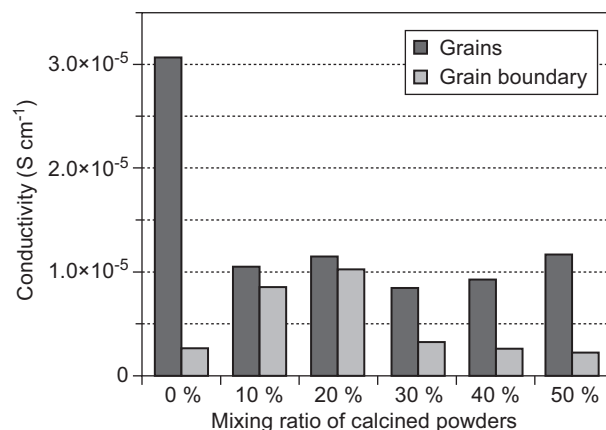
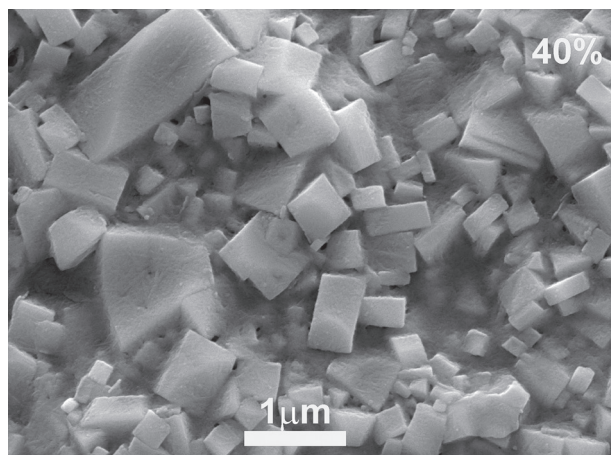


Figure 6. Grains and grain boundary conductivity as a function of mixing ratio.

shape, while for the samples made of 20 - 50 % not-treated powders, the structure was still dense but the morphology showed a mixture of rectangular shaped grains and amorphous regions. The rectangular shapes of the samples mixed with not-treated powders were very different from the spherical shape of the samples with 0 % of not-treated powders. Also the grain sizes became much smaller than those of samples with 0 % of not-treated powders. Similar observation on morphology change was observed by Chang et al. [18] when V was substituted in $\text{Li}_{1+x}\text{Al}_x\text{Ti}_{2-x}\text{P}_3\text{O}_{12}$ and by Norhaniza et al. [17] when Cr and V was doped into $\text{LiSn}_2\text{P}_3\text{O}_{12}$. The change of the grain morphology strongly reflects a liquid (or glass) phase formation during sintering [4]. The relative densities of samples made of 0, 20, 40 and 60 % of not-treated powders were measured as 78, 83, 82 and 81 %. The relative density achieved the maximum at 20 % of not-treated powders.

Besides the grains morphology change, the grains sizes were reduced greatly when mixed with less crystallized powders. For the sample made of 0 % not-treated powders, the grain size was in the range of



c)

Figure 5. SEM micrograph of the cross-sections of $\text{Li}_{1.2}\text{Al}_{0.2}\text{Sn}_{1.8}(\text{PO}_4)_3$ with varied ratios of not-treated powders.

1 - 2 μm . While for the samples mixed with not-treated powders, the size for the well-defined grains was less than 1 μm . The amorphous areas seemed to increase with the amount of not-treated powders.

To better understand the mixing effect of not-treated powders and treated powders, the grain conductivity and grain-boundary conductivity was also plotted separately as a function of mixing ratio of not-treated powders and treated powders. It can be seen from Figure 6 that the grain conductivities of samples made of mixed powders were all lower compared to the sample made of 0 % not-treated powders. The addition of not-treated powders had no positive effects on improving of the grain conductivity. But the trend of the grain boundary conductivities told a different story. The grain-boundary conductivity reached a maximum at 20 %, which indicated an appropriate quantity of not-treated powders, less than 20 % in this case, can enhance the grain-boundary conductivity. This indicated that although the grain conductivity was decreased by the addition of not-treated powders, the enhancement of the grain-boundary conductivity outweighed the negative effect of the addition of not-treated powders on the grain conductivity.

It is speculated that the role of not-treated powders was to act as “bridges” to connect all the treated powders together. These bridges, which helped to form a less-resistive grain boundary by introducing a liquid (or glass) phase during sintering as evidenced by the grain morphology change described previously, facilitated the migration of lithium ions in grain boundaries, thereby resulting in enhanced grain-boundary conductivities. The lower grain conductivity achieved by mixing some not-treated powders is thought due to the lower sinterability of grains originated from those not-treated powders. As the not-treated powders increased further, the increase of grain boundary conductivity due to a less resistive grain boundary was overshadowed by a bigger portion of grain boundary. Nyquist plot of $\text{Li}_{1+x}\text{Al}_x\text{Sn}_{2-x}(\text{PO}_4)_3$ with varied ratios of not-treated powders is shown in Figure 7 for reference.

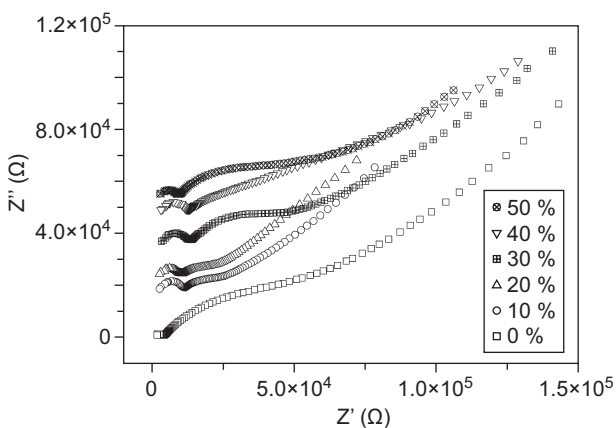


Figure 7. Nyquist plot of $\text{Li}_{1+x}\text{Al}_x\text{Sn}_{2-x}(\text{PO}_4)_3$ with varied ratios of not-treated powders.

CONCLUSIONS

Trivalent Al^{3+} has been doped into $\text{Li}_{1+x}\text{Al}_x\text{Sn}_{2-x}(\text{PO}_4)_3$ systems and the overall conductivity maximized at $x = 0.2$. The enhanced conductivity upon doping of Al^{3+} was attributed to the increased density, a formation of desirable phase with minor impurity and an increase in the mobile Li^+ ion concentration.

The mixing effect of not-treated powders and treated powders has been investigated by varying the mixing ratio of not-treated powders from 0 % to 50 %. The grains morphology of samples with 0 % not-treated powders changed from spherical shapes to rectangular shapes when mixed with not-treated powders, which indicated a liquid (or glass) phase formation during sintering. The overall conductivity peaked at 20 % of not-treated powders. The enhanced overall conductivity was due to the increase of grain boundary conductivity, not the grain conductivity. The reason accounting for the enhanced grain boundary conductivity is attributed to a less-resistive grain boundary as indicated by the grains morphology changes observed.

Acknowledgement

This research was financially supported by the Natural Science Foundation of Hebei Province, China (No.E2013502272), the Fundamental Research Funds for the Central Universities (No. 2015ZD25) and the Scientific Research Foundation for the Returned Overseas Chinese Scholars, State Education Ministry.

REFERENCES

- Knauth P. (2009): Inorganic solid Li ionconductors: an overview. *Solid State Ionics*, 180(14), 911-916. doi:10.1016/j.ssi.2009.03.022.
- Abe T., Ohtsuka M., Sagane F., Iriyama Y., Ogumi Z. (2004): Lithium ion transfer at the interface between lithium-ion-conductive solid crystalline electrolyte and polymer electrolyte. *Journal of the Electrochemical Society*, 151(11), A1950-A1953. doi:10.1149/1.1804813.
- Aono H., Sugimoto E., Sadaoka Y., Imanaka N., Adachi G. (1989): Ionic conductivity of the lithium titanium phosphate ($\text{Li}_{1+x}\text{M}_x\text{Ti}_{2-x}(\text{PO}_4)_3$, M = Al, Sc, Y and La) Systems. *Journal of the Electrochemical Society*, 136(2), 590-591. doi:10.1149/1.2096693.
- Aono H., Sugimoto E., Sadaoka Y., Imanaka N., Adachi G.Y. (1990): Ionic conductivity of solid electrolytes based on lithium titanium phosphate. *Journal of the Electrochemical Society*, 137(4), 1023-1027. doi:10.1149/1.2086597.
- Takada K., Tansho M., Yanase I., Inada T., Kajiyama A., Kouguchi M., Kondo S., Watanabe M. (2001): Lithium ion conduction in $\text{LiTi}_2(\text{PO}_4)_3$. *Solid State Ionics*, 139(3-4), 241-247. doi:10.1016/S0167-2738(01)00688-9
- Fu J. (1997): Superionic conductivity of glass-ceramics in the system $\text{Li}_2\text{O} \cdot \text{Al}_2\text{O}_3 \cdot \text{TiO}_2 \cdot \text{P}_2\text{O}_5$. *Solid State Ionics*, 96(3), 195-200. doi:10.1016/S0167-2738(97)00018-0.

7. Hayashi A., Konishi T., Tadanaga K., Tatsumisago M. (2006): Formation of electrode–electrolyte interface by lithium insertion to $\text{SnS–P}_2\text{S}_5$ negative electrode materials in all-solid-state cells. *Solid State Ionics*, 177 (26), 2737–2740. doi:10.1016/j.ssi.2006.05.021.
8. Murugan R., Thangadurai V., Weppner W. (2007): Fast lithium ion conduction in garnet-type $\text{Li}_7\text{La}_3\text{Zr}_2\text{O}_{12}$. *Angewandte Chemie International Edition*, 46(41), 7778–7781. doi:10.1002/anie.200701144.
9. Kotobuki M., Suzuki Y., Kanamura K., Sato Y., Yamamoto K., Yoshida T. (2011): A novel structure of ceramics electrolyte for future lithium battery. *Journal of Power Source*, 196(22), 9815–9819. doi:10.1016/j.jpowsour.2011.07.005.
10. Zhang M., Huang Z., Cheng J.F., Yamamoto O., Imanishi N., Chi B., Pu J., Li J. (2014): Solid state lithium ionic conducting thin film $\text{Li}_{1.4}\text{Al}_{0.4}\text{Ge}_{1.6}(\text{PO}_4)_3$ prepared by tape casting. *Journal of Alloys and Compounds*, 590, 147–152. doi:10.1016/j.jallcom.2013.12.100.
11. Narváez-Semanate J.L. and Rodrigues A.C.M. (2010): Microstructure and ionic conductivity of $\text{Li}_{1+x}\text{Al}_x\text{Ti}_{2-x}(\text{PO}_4)_3$ NASICON glass-ceramics. *Solid State Ionics*, 181(25), 1197–1204. doi:10.1016/j.ssi.2010.05.010.
12. Mei A., Wang X.L., Lan J.L., Feng Y.C., Geng H.X., Lin Y.H., Nan C.W. (2010): Role of amorphous boundary layer in enhancing ionic conductivity of lithium–lanthanum–titanate electrolyte. *Electrochimica Acta*, 55(8), 2958–2963. doi:10.1016/j.electacta.2010.01.036.
13. Kim, H.-S., Choi K.S., Kim E.J (2015): Characterization of Sputter-Deposited $\text{LiZr}_2(\text{PO}_4)_3$ Thin Film Solid Electrolyte, *Journal of the electrochemical society*, 162(10), A2080–A2084. doi:10.1149/2.0501510jes
14. El-Shinawi H., Greaves C., Janek J. (2015): Sol-gel synthesis and room-temperature properties of alpha- $\text{LiZr}_2(\text{PO}_4)_3$, *RSC Advances*, 5(22), 17054–17059. doi:10.1039/C4RA16804F
15. Chung H., Kang B. (2014): Increase in grain boundary ionic conductivity of $\text{Li}_{1.5}\text{Al}_{0.5}\text{Ge}_{1.5}(\text{PO}_4)_3$ by adding excess lithium. *Solid State Ionics*, 263, 125–130. doi:10.1016/j.ssi.2014.05.016.
16. Norhaniza R., Subban R.H.Y., Mohamed N.S., Ahmad A. (2012): Chromium substituted $\text{LiSn}_2\text{P}_3\text{O}_{12}$ solid electrolyte. *International Journal of Electrochemical Science*, 7, 10254–10265.
17. Norhaniza R., Subban R.H.Y., Mohamed N.S. (2013): Cr and V substituted $\text{LiSn}_2\text{P}_3\text{O}_{12}$ solid electrolyte materials. *Journal of Power Source*, 244, 300–305. doi:10.1016/j.jpowsour.2012.12.119.
18. Chang C.M., Lee Y.I., Hong S.H. (2005): Spark plasma sintering of $\text{LiTi}_2(\text{PO}_4)_3$ -based solid electrolytes, *Journal of the American Ceramics Society*, 88(7), 1803–1807. doi:10.1111/j.1551-2916.2005.00246.x.